Journal of Engineering Science and Technology Review 16 (4) (2023) 205 - 213

Research Article

JOURNAL OF
Engineering Science and Technology Review

www.jestr.org

Analysis on Vehicle-bridge Coupled Random Vibration under the Action of Heavy Vehicle Considering Non-uniform Effect

Na Zhu[1, 2, *] and Shuisheng Chen[1]

[1]*School of Civil Engineering and Architecture, East China Jiaotong University, Nanchang 330013, China*
[2]*School of Civil and Architecture Engineering, Nanchang Institute of Technology, Nanchang 330099, China*

Received 3 June 2023; Accepted 18 August 2023

Abstract

In the highway vehicle-bridge coupling random vibration analysis, only the input model of uniform effect under the complete incoherence of vehicle wheels is generally considered but neglecting the influence of non-uniform effect triggered by road irregularity excitation on vibration response. To accurately judge the dynamic response and frequency spectrum characteristics of the bridge when the heavy vehicle was excited by the road surface, a vehicle-bridge coupling random vibration model of a six-axle heavy vehicle under multi-point coherent excitation was established on the basis of the structural dynamical principle and the pseudo-excitation method, and a 30-m simply supported T-beam bridge model was constructed through finite element analysis. Then, the random dynamic response and frequency spectrum characteristics of the bridge considering the non-uniform effect of the road surface spectrum under the influence of speed were analyzed and compared with those only considering the uniform effect. Results show that the response value of bridge mid-span under the action of a six-axle heavy vehicle is obviously lower than that under the uniform effect, especially at a speed of 50km/h, the maximum root mean square (RMS) values of the displacement and acceleration of the former are only 0.299 times and 0.348 times those of the latter. When the maximum response occurs, the position of the front wheel of the vehicle is different from that under the same speed and only considering the uniform effect. When the vehicle is driving at low speed and high speed, the number of main frequencies of the bridge considering the non-uniform effect increases, and the amplitude of power spectral density (PSD) is highly reduced compared with that considering the uniform effect. At the speed of 120km/h, the number of main frequencies increases from 2 under the uniform effect to 4. Conclusions obtained in the study have a significantly academic value for the application of heavy vehicle in the research on bridge reliability.

Keywords: Six-axle heavy vehicle, Pseudo-excitation method, Non-uniform effect, Random vibration, Simply supported T-beam

1. Introduction

The random vibration generated by bridge deck irregularity excitation is the main cause of bridge vibration [1]. The randomness of bridge deck irregularity will lead to random bridge vibration, thereby also causing the randomness in the bridge vibration frequency. Meanwhile, the bridge vibration intensity becomes uncertain. In general, the vibration frequency and vibration intensity of bridges are studied by establishing the vehicle-bridge coupling random vibration models. The vehicle-bridge coupling random vibration analysis is crucial to the research on the reliability of bridge structures.

However, while investigating the vehicle-bridge coupling random vibration response, the types of heavy vehicles have undergone evident changes due to the development of China's transportation. The vehicle-bridge coupling model will be affected by heavy vehicle parameters, the number of vehicle axles and wheels, and the input of the wheel excitation model under bridge deck irregularity. By contrast, the dynamic performance of bridges will be directly influenced by the accuracy of the established vehicle-bridge coupling excitation model.

At present, the main methods used to study the random vibration of bridges are the Monte Carlo method, covariance analysis method, evolutionary random method, and pseudo-excitation method. Among them, the Monte Carlo method [2] calculates the vibration response of bridges by simulating a sample with certain road irregularity [3]. Ensuring the accuracy of the calculation results requires a lot of calculation time with low calculation efficiency. Concerning the pseudo-excitation method [4] proposed by Dalian University of Technology in China, a series of virtual harmonic excitations are constructed by inputting the power spectrum on the premise of the known power spectrum density of random excitation, which transforms the calculation of stationary random vibration into the calculation of steady-state harmonic response. The latter solves the random vibration response in the frequency domain and better reflects the randomness of vibration with high calculation efficiency. The pseudo-excitation method has been extensively used in the research field of random bridge vibration excited by earthquake and track irregularity and less involved in the analysis of vehicle-bridge coupling random vibration. On establishing the vehicle-bridge coupling system model, the vehicle-bridge coupling model of multi-axle heavy vehicles was established according to the principle of structural dynamics [5-8], which simulated vehicle crossing and actual vehicle-bridge interaction more accurately than the single-degree-of-freedom vehicle model proposed in the early stage [9], thus,

*E-mail address: 260418694@qq.com
ISSN: 1791-2377
doi:10.25103/jestr.164.25

the random bridge response analysis conformed better to the actual situation. However, research has scarcely investigated the vehicle-bridge coupling models of six-axle heavy vehicles as the numbers of heavy axles have been transformed from the initial two-axle heavy vehicles [10] into the leading six-axle heavy vehicles. As for the research considering the wheel coherence under road surface excitation, the uniform effect under wheel incoherence was initially ignored; then, only the time lag effect of front and rear wheels was considered; finally, the coherent effect considering both front and rear wheels and left and right wheels was investigated. However, most of such studies have been merely restricted to the time domain, and the highway vehicle-bridge coupling random vibration response has been rarely explored through the pseudo-excitation method within the frequency domain.

On this basis, researchers have conducted a substantial amount of fundamental research work on vehicle-bridge coupling random vibration response. Nonetheless, Monte Carlo time domain analysis plays a dominant role when solving the random vibration of bridges under the excitation of bridge deck irregularity, but analysis is lacking in the frequency domain, not to mention the non-uniform effect considering wheel excitation. Therefore, research has scarcely investigated the influence of the non-uniform effect on random bridge vibration within the frequency range, thereby necessitating the establishment of a vehicle-bridge coupling excitation model of six-axle heavy vehicles and study of the bridge vibration response under the road surface non-uniform effect within the frequency domain. In this study, a vehicle-bridge coupling pseudo-excitation model under the action of a six-axle heavy vehicle was established on the basis of the structural dynamical principle and pseudo-excitation method. Moreover, the influences of the speed change on the bridge random vibration and spectrum characteristics considering the non-uniform effect were analyzed and compared with the bridge random vibration only considering the uniform effect. This study aims to determine the random vibration response of a simply supported beam bridge under the action of a six-axle heavy vehicle and to gain better mastery on the dynamic performance of the bridge.

2. State of the art

For a long time, many scholars have studied vehicle-bridge coupling random vibration. B. Nunia [11] analyzed the influence of the maximum vertical acceleration of the bridge with the change in prestress in the beam under bridge deck irregularity excitation, explored the impact factor of the simply supported beam bridge with different spans under the action of the train composed of four- and two-axle vehicles, considered the influence of the vehicle speed [12], and deemed that the vertical acceleration at the bridge mid-span was directly proportional to the bridge stiffness except for a few spans. O. Mohammed [13] compared the 19-axle long heavy vehicle with the 5-axle vehicle and found that the maximum impact factor of the long heavy vehicle was less than that of the 5-axle vehicle under the same road grade. H. Ho [14] concluded that the maximum vertical acceleration response of the bridge increased with the increase in vehicle speed, when the random traffic flow composed of two-axle vehicles passes a simply supported beam bridge. G. Alencar [15] evaluated the fatigue life considering vehicle-bridge coupling random vibration when a two-axle vehicle acted on a steel-concrete simply supported bridge. In all of the above studies, the random vibration response analysis has been performed using the Monte Carlo method within the time domain, and only the uniform effect of wheel excitation has been considered. Taking a simply supported plate girder bridge as example, J. Oliva [16] considered the coherence of left and right wheels and that of four wheels, respectively, and established a new road surface roughness coherence equation with 10 road surface irregularity samples. The results showed that at the mid-span of the simply supported plate girder bridge, the impact factor under four-wheel coherence was smaller than that under two-wheel coherence; additionally, analyzing the random vibration response continued within the time domain, although the non-uniform effect of wheel excitation was considered. C. C. Caprani [17] investigated the random response at the mid-span of a footbridge through the pseudo-excitation method and considered the influence of different walk models on the maximum RMS of acceleration response at the bridge mid-span. The non-uniform effect of excitation was not considered, although this study was carried out within the frequency domain. S. Tamaddon [18] investigated the influence of non-uniform vertical excitation under earthquake action on the impact phenomenon of a concrete continuous curved bridge and pointed out that when the ratio of vertical acceleration to horizontal acceleration under the non-uniform effect was a certain value, the displacement response of the bridge was 21% greater than that under the uniform effect. Taking a long-span suspension bridge as example, H. Tang [19] concluded that the flutter stability of the bridge tended to deteriorate easily after the non-uniform effect of wind vibration was considered. According to the pseudo-excitation method, G. Bethel Lulu [20] explored track-bridge coupling vibration considering the vertical vibration response of the rail track under the non-uniform effect of wheels. C. Ma [21] studied the influence of seismic wave on random bridge vibration and deemed that the maximum acceleration response of the bridge could increase or decline after the non-uniform effect was considered. In all of the above studies, the pseudo-excitation method has been used, considering wind vibration and seismic action within the frequency domain, the wheel-track excitation, as well as the non-uniform effect of excitation; whereas research rarely examined the road surface irregularity excitation under the highway vehicle-bridge coupling vibration. Z. Zembaty [22] concluded that owing to the existence of phase difference or coherence, the response caused by each excitation may be superposed or may offset each other, namely, the result of the random bridge vibration response considering the non-uniform effect may be lower or higher than the effect under the uniform effect. Hence, the random bridge response under the non-uniform effect will be affected by the number of vehicle wheels, wheel spacing, and bridge type.

Given the deficiency of the existing research, the load caused by road surface irregularity was equivalent to pseudo-excitation; a typical six-axle heavy vehicle model was selected, and a 30-m span prefabricated prestressed concrete simply supported T-beam bridge widely used in highway was taken as the object to study the influence of the non-uniform effect of wheel excitation on vehicle-bridge coupling vibration response and frequency spectrum characteristics. The paper aims to provide a basis for the reliability research and analysis of bridges under the action of heavy vehicles in the future.

The remainder of this study is organized as follows: Section III establishes a vehicle-bridge coupling system

model through the pseudo-excitation method based on the principle of dynamics. Section IV analyzes an example, followed by the bridge vibration response analysis considering the non-uniform effect of wheel excitation. The final section summarizes the whole paper and draws relevant conclusions.

3. Methodology

3.1 Vehicle-bridge coupling system modeling

3.1.1 Vehicle model

Based on several national highway traffic surveys, dynamic weighing data, and existing research results, six-axle vehicles are the most common freight vehicles at present, and the vehicle dynamic analysis model refers to [23]. The whole vehicle can be divided into 14 rigid parts: 2 car bodies and 12 wheels, and the total number of independent degrees of freedom of the vehicle are 17. Vehicle vibration equation is written as (1):

$$\boldsymbol{M}_v\ddot{\boldsymbol{z}}+\boldsymbol{C}_v\dot{\boldsymbol{z}}+\boldsymbol{K}_v\boldsymbol{z}=\boldsymbol{F}_v^{int} \tag{1}$$

$$F_{v,i}^{int}=k_{ti}d_{vb,i}+c_{ti}\dot{d}_{vb,i} \tag{2}$$

$$d_{vb,i}=z_i-r_i-y_i \tag{3}$$

where $\boldsymbol{M}_v$, $\boldsymbol{C}_v$ and $\boldsymbol{K}_v$ are the mass, damping, and stiffness matrices of the vehicle, respectively, $\boldsymbol{F}_v^{int}$ represents the inertial load generated by the vehicle, $F_{v,i}^{int}$ is the inertial load generated by each degree of freedom of the vehicle, and $\boldsymbol{z}$ is the degree of freedom vector of the vehicle model, $\boldsymbol{z}=\{Z_{vaL}^1,Z_{vaR}^1,Z_{vaL}^2,Z_{vaR}^2,Z_{vaL}^3,Z_{vaR}^3,Z_{vaL}^4,Z_{vaR}^4,Z_{vaL}^5,Z_{vaR}^5,Z_{vaL}^6,Z_{vaR}^6,Z_{vr}^1,\theta_{vr}^1,\phi_{vr}^1,Z_{vr}^2,\phi_{vr}^2\}^T$

in which Z_{vr}^1, θ_{vr}^1 and ϕ_{vr}^1 are the vertical displacement, rotation around Y axis, and side roll around X axis of the tractor, respectively, Z_{vr}^2 and ϕ_{vr}^2 represent the vertical displacement and the rotation of the trailer around the Y axis, respectively, Z_{vaL}^k and Z_{vaR}^k $(k=1,2,3,4,5,6)$ denote the vertical displacement of the left and right wheels of the k -th axle, respectively, L and R stand for the left and right rigid bodies of the X axis,the subscript vr indicates the vehicle body, a represents the suspension, and $d_{vb,i}(i=1,2,3...,12)$ is the vertical displacement of the i -th wheel relative to the bridge deck, y_i is the initial vertical displacement of the bridge deck slab at the wheel i, r_i is theroad surface irregularity value at the wheel i, z_i is the vertical displacement of the i -th wheel.

3.1.2 Bridge model

The bridge was discretized using finite elements, and its vibration equation is as follows:

$$\boldsymbol{M}_b\ddot{\boldsymbol{y}}+\boldsymbol{C}_b\dot{\boldsymbol{y}}+\boldsymbol{K}_b\boldsymbol{y}=-\boldsymbol{F}_{bv}^{int}-\boldsymbol{F}_g \tag{4}$$

where $\boldsymbol{F}_{bv}^{int}$ denotes the inertial force vector acted by vehicle vibration on the bridge deck, $\boldsymbol{F}_g$ represents the static load vector acted by each wheel on the bridge deck slab and caused by the vehicle gravity, $\boldsymbol{y}$ is the nodal vector ,and $\boldsymbol{M}_b$ $\boldsymbol{C}_b$ and $\boldsymbol{K}_b$ are the mass, damping, and stiffness matrix of the bridge, respectively.

To reduce the calculation workload, the modal comprehensive superposition technology was introduced, Rayleigh damping was used, and the r -order mode was taken. According to the mode decomposition method, Equation (4) can be rewritten as follows:

$$\boldsymbol{I}\ddot{\boldsymbol{q}}+\boldsymbol{X}\dot{\boldsymbol{q}}+\boldsymbol{\Omega}\boldsymbol{q}=-\Phi^T(\boldsymbol{F}_{bv}^{int}+\boldsymbol{F}_g) \tag{5}$$

where $\boldsymbol{I}$, $\boldsymbol{X}$, $\boldsymbol{\Omega}$ are the diagonal mass, damping, and stiffness matrices, respectively, $\boldsymbol{\Phi}$ is the r -order modal vector matrix of the bridge, $\boldsymbol{\Phi}=[\phi_1,\phi_2,\ldots,\phi_r]$, ϕ_r is the modal vector of each node corresponding to the r -order frequency. $\boldsymbol{q}$ is the generalized coordinate vector of the bridge.

3.1.3 Vehicle-bridge coupling model

The wheels and the bridge deck are assumed to remain together when the vehicle is running, and the vehicle and the bridge are connected through the displacement coordination and the balance condition of the interaction force at the contact point between the wheels and the bridge deck. The interaction force between the i -th wheel and the bridge can be expressed as follows:

$$F_{v,i}^{int}=-F_{bv,i}^{int} \tag{6}$$

A vehicle-bridge coupling vibration equation can be established by substituting (2)、(3)and (6) into (5) combined with simultaneous Equations (1):

$$\boldsymbol{M}_{bv}\ddot{\boldsymbol{u}}+\boldsymbol{C}_{bv}\dot{\boldsymbol{u}}+\boldsymbol{K}_{bv}\boldsymbol{u}=\boldsymbol{F}_g+\boldsymbol{F}_w \tag{7}$$

where $\boldsymbol{M}_{bv}$, $\boldsymbol{C}_{bv}$ and $\boldsymbol{K}_{bv}$ are the mass, damping, and stiffness matrices of the vehicle-bridge coupling vibration model, respectively, $\boldsymbol{u}$ is the vehicle-bridge coupling generalized coordinate vector, $\boldsymbol{u}=\{q_1,q_2,\ldots,q_r,Z_{vaL}^1,Z_{vaR}^1,\ldots,Z_{vaL}^6,Z_{vaR}^6,Z_{vr}^1,\theta_{vr}^1,\phi_{vr}^1,Z_{vr}^2,\phi_{vr}^2\}^T$, and $\boldsymbol{F}_g$ is the deterministic excitation caused by the axle load of the vehicle, $\boldsymbol{F}_w$ is the random excitation triggered by bridge deck irregularity. When only the action of the random excitation caused by road surface irregularity $\boldsymbol{F}_w$ was considered, the vibration equation of the vehicle-bridge coupling time-varying system could be written as:

$$\boldsymbol{M}_{bv}\ddot{u}''+\boldsymbol{C}_{bv}\dot{u}''+\boldsymbol{K}_{bv}\boldsymbol{u}''=\boldsymbol{F}_w \tag{8}$$

where $\boldsymbol{u}''$ is the generalized coordinate vector of vehicle-bridge coupling vibration caused by the excitation of road surface irregularity.

3.2 Vehicle-bridge coupling pseudo-excitation model

3.2.1 Coherent effect model of road surface excitation

The excitation of road surface irregularity input into each wheel is affected by the road roughness coefficient, left-right wheel spacing, and left-right wheel coherence function. For the vibration transmission input by the 12 wheels of the heavy vehicle, the self-spectra of the 12 wheels and the cross-spectra between them, totaling 144 spectra (12 self-spectra and 132 cross-spectra) should be calculated. The PSD matrix input by the road surface excitation under the coherent effect of the six-wheel vehicle was deduced as seen in Equation (9):

$$\boldsymbol{G}_q(\omega)=G_q(\omega)\begin{bmatrix}
1 & coh(n) & e^{-j2\pi nL_{1-3}} & coh(n)e^{-j2\pi nL_{1-3}} & e^{-j2\pi nL_{1-5}} & coh(n)e^{-j2\pi nL_{1-5}} & e^{-j2\pi nL_{1-7}} & coh(n)e^{-j2\pi nL_{1-7}} & e^{-j2\pi nL_{1-9}} & coh(n)e^{-j2\pi nL_{1-9}} & e^{-j2\pi nL_{1-11}} & coh(n)e^{-j2\pi nL_{1-11}} \\
coh(n) & 1 & coh(n)e^{-j2\pi nL_{1-3}} & e^{-j2\pi nL_{1-3}} & coh(n)e^{-j2\pi nL_{1-5}} & e^{-j2\pi nL_{1-5}} & coh(n)e^{-j2\pi nL_{1-7}} & e^{-j2\pi nL_{1-7}} & coh(n)e^{-j2\pi nL_{1-9}} & e^{-j2\pi nL_{1-9}} & coh(n)e^{-j2\pi nL_{1-11}} & e^{-j2\pi nL_{1-11}} \\
e^{j2\pi nL_{1-3}} & coh(n)e^{j2\pi nL_{1-3}} & 1 & coh(n) & e^{-j2\pi nL_{3-5}} & coh(n)e^{-j2\pi nL_{3-5}} & e^{-j2\pi nL_{3-7}} & coh(n)e^{-j2\pi nL_{3-7}} & e^{-j2\pi nL_{3-9}} & coh(n)e^{-j2\pi nL_{3-9}} & e^{-j2\pi nL_{3-11}} & coh(n)e^{-j2\pi nL_{3-11}} \\
coh(n)e^{j2\pi nL_{1-3}} & e^{j2\pi nL_{1-3}} & coh(n) & 1 & coh(n)e^{-j2\pi nL_{3-5}} & e^{-j2\pi nL_{3-5}} & coh(n)e^{-j2\pi nL_{3-7}} & e^{-j2\pi nL_{3-7}} & coh(n)e^{-j2\pi nL_{3-9}} & e^{-j2\pi nL_{3-9}} & coh(n)e^{-j2\pi nL_{3-11}} & e^{-j2\pi nL_{3-11}} \\
e^{j2\pi nL_{1-5}} & coh(n)e^{j2\pi nL_{1-5}} & e^{j2\pi nL_{3-5}} & coh(n)e^{j2\pi nL_{3-5}} & 1 & coh(n) & e^{-j2\pi nL_{5-7}} & coh(n)e^{-j2\pi nL_{5-7}} & e^{-j2\pi nL_{5-9}} & coh(n)e^{-j2\pi nL_{5-9}} & e^{-j2\pi nL_{5-11}} & coh(n)e^{-j2\pi nL_{5-11}} \\
coh(n)e^{j2\pi nL_{1-5}} & e^{j2\pi nL_{1-5}} & coh(n)e^{j2\pi nL_{3-5}} & e^{j2\pi nL_{3-5}} & coh(n) & 1 & coh(n)e^{-j2\pi nL_{5-7}} & e^{-j2\pi nL_{5-7}} & coh(n)e^{-j2\pi nL_{5-9}} & e^{-j2\pi nL_{5-9}} & coh(n)e^{-j2\pi nL_{5-11}} & e^{-j2\pi nL_{5-11}} \\
e^{j2\pi nL_{1-7}} & coh(n)e^{j2\pi nL_{1-7}} & e^{j2\pi nL_{3-7}} & coh(n)e^{j2\pi nL_{3-7}} & e^{j2\pi nL_{5-7}} & coh(n)e^{j2\pi nL_{5-7}} & 1 & coh(n) & e^{-j2\pi nL_{7-9}} & coh(n)e^{-j2\pi nL_{7-9}} & e^{-j2\pi nL_{7-11}} & coh(n)e^{-j2\pi nL_{7-11}} \\
coh(n)e^{j2\pi nL_{1-7}} & e^{j2\pi nL_{1-7}} & coh(n)e^{j2\pi nL_{3-7}} & e^{j2\pi nL_{3-7}} & coh(n)e^{j2\pi nL_{5-7}} & e^{j2\pi nL_{5-7}} & coh(n) & 1 & coh(n)e^{-j2\pi nL_{7-9}} & e^{-j2\pi nL_{7-9}} & coh(n)e^{-j2\pi nL_{7-11}} & e^{-j2\pi nL_{7-11}} \\
e^{j2\pi nL_{1-9}} & coh(n)e^{j2\pi nL_{1-9}} & e^{j2\pi nL_{3-9}} & coh(n)e^{j2\pi nL_{3-9}} & e^{j2\pi nL_{5-9}} & coh(n)e^{j2\pi nL_{5-9}} & e^{j2\pi nL_{7-9}} & coh(n)e^{j2\pi nL_{7-9}} & 1 & coh(n) & e^{-j2\pi nL_{9-11}} & coh(n)e^{-j2\pi nL_{9-11}} \\
coh(n)e^{j2\pi nL_{1-9}} & e^{j2\pi nL_{1-9}} & coh(n)e^{j2\pi nL_{3-9}} & e^{j2\pi nL_{3-9}} & coh(n)e^{j2\pi nL_{5-9}} & e^{j2\pi nL_{5-9}} & coh(n)e^{j2\pi nL_{7-9}} & e^{j2\pi nL_{7-9}} & coh(n) & 1 & coh(n)e^{-j2\pi nL_{9-11}} & e^{-j2\pi nL_{9-11}} \\
e^{j2\pi nL_{1-11}} & coh(n)e^{j2\pi nL_{1-11}} & e^{j2\pi nL_{3-11}} & coh(n)e^{j2\pi nL_{3-11}} & e^{j2\pi nL_{5-11}} & coh(n)e^{j2\pi nL_{5-11}} & e^{j2\pi nL_{7-11}} & coh(n)e^{j2\pi nL_{7-11}} & e^{j2\pi nL_{9-11}} & coh(n)e^{j2\pi nL_{9-11}} & 1 & coh(n) \\
coh(n)e^{j2\pi nL_{1-11}} & e^{j2\pi nL_{1-11}} & coh(n)e^{j2\pi nL_{3-11}} & e^{j2\pi nL_{3-11}} & coh(n)e^{j2\pi nL_{5-11}} & e^{j2\pi nL_{5-11}} & coh(n)e^{j2\pi nL_{7-11}} & e^{j2\pi nL_{7-11}} & coh(n)e^{j2\pi nL_{9-11}} & e^{j2\pi nL_{9-11}} & coh(n) & 1
\end{bmatrix} \tag{9}$$

where $G_q(\omega)$ stands for the PSD matrix, L_{g-h} represents the wheel spacing, and the subscript $g-h$ $(g=1,3,5,7,9 h=3,5,7,9,11)$ is the spacing between two wheels on the same side, $coh(n)$ is the universal frequency domain model [24], and the value of the coherence function is only related to the wheel spacing and vehicle speed, that is:

$$coh(n)=e^{-\omega B/v} \tag{10}$$

where B is the left-right wheel spacing, v is the vehicle running speed, $\omega=2\pi n$, and n represents the spatial frequency.

If the coherence of the left and right wheel tracks excited by the spectral excitation input on the road surface is not considered, then, the road spectral coherence function is $coh(n)=0$, that is, only the time lag effect of the road spectrum on the front and rear wheel is considered, and Equation (9) can be rewritten as the input power spectrum matrix input of the time lag effect, which is hereby omitted.

3.2.2 Vehicle-bridge coupling pseudo-excitation load model and response analysis

In general, the road surface irregularity input matrix considering the road surface coherent effect and time lag effect cannot be generally decomposed into the multiplication form of two vectors. Considering that the power spectrum matrix must be a nonnegative definite Hermit matrix [25], however, it can be expressed through the following form:

$$\boldsymbol{G}_{q1}(\omega)=\sum_{j=1}^{m}\lambda_j\boldsymbol{\psi}_j^*\boldsymbol{\psi}_j^T(m=12) \tag{11}$$

where complex conjugate and matrix (vector) transpositions are taken for the superscripts * and T, $\boldsymbol{G}_{q1}(\omega)$ is the Hermit matrix, λ_j and $\boldsymbol{\psi}_j$ represent the Eigen value and feature pair of the Hermit matrix, respectively. Therefore, constructing the following pseudo-excitation is only necessary using the features of each order:

$$\tilde{p}_j=\boldsymbol{\psi}_j^*\sqrt{\lambda_j}e^{i\omega t} \tag{12}$$

$\boldsymbol{G}_{q1}(\omega)$ can be expressed through the following form:

$$\boldsymbol{G}_{q1}(\omega)=\sum_{j=1}^{m}\tilde{\boldsymbol{p}}_j^*\tilde{\boldsymbol{p}}_j^T \tag{13}$$

$$\boldsymbol{M}_{bv}\ddot{\tilde{\boldsymbol{u}}}(\omega,t)+\boldsymbol{C}_{bv}\dot{\tilde{\boldsymbol{u}}}(\omega,t)+\boldsymbol{K}_{bv}\tilde{\boldsymbol{u}}(\omega,t)=\tilde{\boldsymbol{F}}_w(\omega,t) \tag{14}$$

Equation (14) is iteratively solved using the Newmark-β integral form, and the pseudo response is calculated to determine the power spectrum matrix of the system response.

$$S_{uu}(\omega,t)=\sum_{j=1}^{m}\tilde{\boldsymbol{u}}^*(\omega,t)\tilde{\boldsymbol{u}}^T(\omega,t) \tag{15}$$

$$\sigma_{yy}^2(t)=\int_{-\infty}^{+\infty}S_{uu}(\omega,t)d\omega \tag{16}$$

where $S_{uu}(\omega,t)$ is the function of PSD, and $\sigma_{yy}^2(t)$ stands for the standard deviation of the random vibration response.

4. Results analysis and discussion

4.1 Example analysis

4.1.1 Dynamic characteristic parameters of the vehicle and bridge

(1) Vehicle parameters

The spacing and axle data and the dynamic parameters of the vehicle were selected as seen in Tables 1 and 2 [23]. For the excitation of bridge deck irregularity excitation, the power system on the wheel, C_{vlL}^i stands for the equivalent tire damping, K_{vuL}^i is the spring stiffness of the suspension system on the wheel, and K_{vlL}^i represents the equivalent tire stiffness.

spectrum of Grade B road surface (the road roughness coefficient of Grade B road surface: $G_q(n_0)=64\times10^{-6}mm^2\cdot m$) suggested in GB7301-2005 was chosen.

In Table 1, C_{vuL}^i is the damping of the suspension

Table 1. Parameters of the six-axle tractor trailer vehicle model

	Spring stiffness (KN/m)		**Spring damper** ($KN{\cdot}s/m$)		**Other parameters**		
	Parameter	**Value**	**Parameter**	**Value**	**Parameter**	**Value**	
Suspension Part	$K_{vuL}^1 = K_{vuR}^1$	350	$C_{vuL}^1 = C_{vuR}^1$	20	Mass of tractor	7,000 (kg)	
	$K_{vuL}^2 = K_{vuR}^2$	500	$C_{vuL}^2 = C_{vuR}^2$	60	Pitching moment of inertia of tractor	4,604 ($kg{\cdot}m^2$)	
	$K_{vuL}^3 = K_{vuR}^3$	500	$C_{vuL}^3 = C_{vuR}^3$	60	Rolling moment of inertia of tractor	8,544 ($kg{\cdot}m^2$)	
	$K_{vuL}^4 = K_{vuR}^4$	400	$C_{vuL}^4 = C_{vuR}^4$	60	Mass of tractor	38,770 (kg)	
	$K_{vuL}^5 = K_{vuR}^5$	400	$C_{vuL}^5 = C_{vuR}^5$	60	Pitching moment of inertia of trailer	16,300 (kg)	
	$K_{vuL}^6 = K_{vuR}^6$	400	$C_{vuL}^6 = C_{vuR}^6$	60	Rolling moment of inertia of trailer	181,216 ($kg{\cdot}m^2$)	
Tire Part	$K_{vlL}^1 = K_{vlR}^1$	1,000	$C_{vlL}^1 = C_{vlR}^1$	10	Spacing	$L_1 = 1.65(m)$	$L_7 = 1.3(m)$
	$K_{vlL}^2 = K_{vlR}^2$	2,000	$C_{vlL}^2 = C_{vlR}^2$	20		$L_2 = 1.65(m)$	$L_8 = 2.4(m)$
	$K_{vlL}^3 = K_{vlR}^3$	2,000	$C_{vlL}^3 = C_{vlR}^3$	20		$L_3 = 1.3(m)$	$L_9 = 5.6(m)$
	$K_{vlL}^4 = K_{vlR}^4$	2,000	$C_{vlL}^4 = C_{vlR}^4$	20		$L_4 = 5(m)$	
	$K_{vlL}^5 = K_{vlR}^5$	2,000	$C_{vlL}^5 = C_{vlR}^5$	20		$L_5 = 2.3(m)$	
	$K_{vlL}^6 = K_{vlR}^6$	2,000	$C_{vlL}^6 = C_{vlR}^6$	20		$L_6 = 1.3(m)$	

In Table 2, f_k denotes the wheel load, the total load mass is 48.85 t, and the weights from the first to the six axles are 7t, 9t, 9t, 7.95t, and 7.95 t, respectively.

Table 2. Parameters of the six-axle tractor trailer vehicle model

Wheel Weight (N)
$f_1 = f_2 = 34300$
$f_3 = f_4 = f_5 = f_6 = 44100$
$f_7 = f_8 = f_9 = f_{10} = f_{11} = f_{12} = 38955$

(2) Bridge structure parameters

A prestressed concrete simply supported T-beam bridge with a standard span of 30-m used in highway was selected. The bridge deck had a clear width of 11m (one of the two-way separated bridges) with two lanes. The load level of bridge is highway-I. Both prefabricated and cast-in-place concrete are C50. The cross section was composed of 5 T-beams with 5 transverse diaphragm beams whose cross-sectional layout is as shown in Fig. 1. According to the design data of the bridge, the refined model of the bridge was established through ANSYS as shown in Fig. 2 in which the main beam and diaphragm beams were simulated using solsh190 solid elements, the bridge deck pavement was simulated using shell181 plate elements, and the bridge pavement was connected with the main beam through contact. The T-beam bridge deck was taken as the target surface simulated using TARGE170 elements, and bridge deck pavement as the contact surface was simulated using CONTA15 elements. The refined modeling was performed using T-beam+ pavement layer+ anti-collision wall. The bridge model totally contained 7,871 elements, among which 4,947 were T-beam elements; 2,610 were bridge pavement elements; and 232 were anti-collision wall elements. Table 3 presents the first ten orders of vibration frequencies of the bridge.

4.1.2 Vehicle loading

According to the driving characteristics of vehicles on the bridge and the provisions on transverse vehicle load distribution in the *Technical Specification for Construction of Highway Bridge and Culvert*, the vehicle ran under the normal conditions of the lane. Fig. 3 displays the vehicle loading layout.

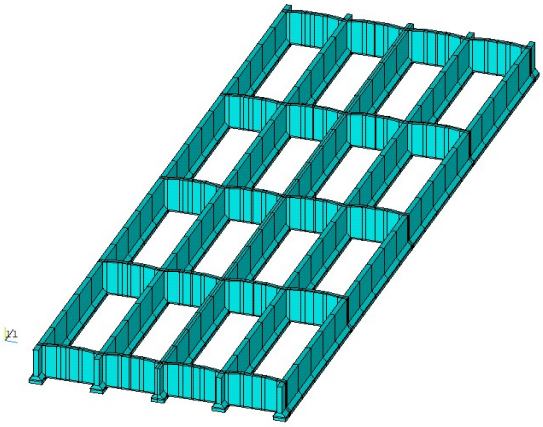

Fig. 1. Diaphragm beam layout

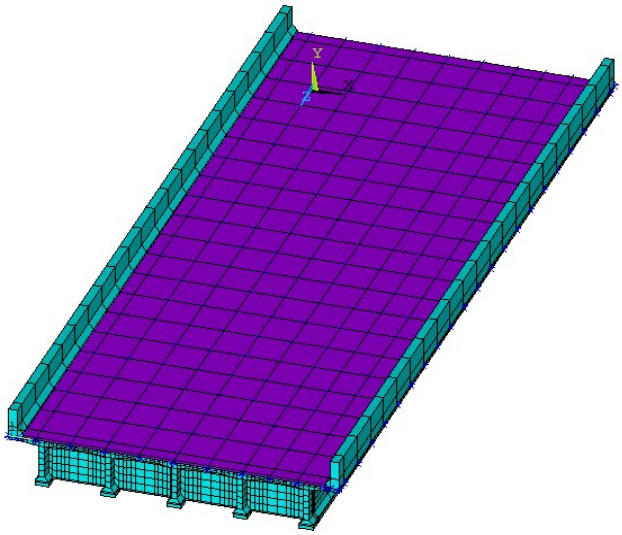

Fig. 2. Bridge entity finite element model

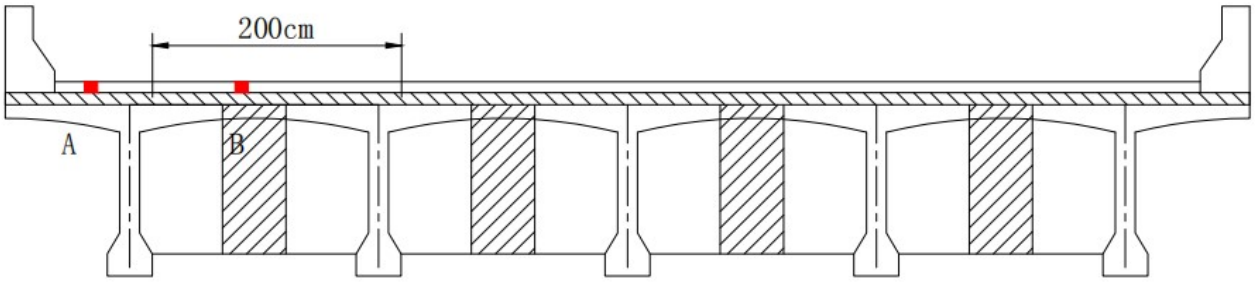

Fig. 3. Typical cross section of 30-m T-beam

Table 3. Frequencies and model of the first ten modes

Mode	Natural frequencies (*Hz*)	Shape description
First	4.21	Symmetrical vertical bending
Second	5.94	Anti-symmetry torsion
Third	13.40	Anti-symmetry vertical bending
Fourth	14.37	Anti-symmetry torsion+ Lateral bending
Fifth	17.27	Symmetrical vertical bending+ Symmetrical torsion
Sixth	17.49	Anti-symmetry vertical bending+ Anti-symmetry torsion
Seventh	18.88	Anti-symmetry vertical bending+ Deck torsion
Eighth	22.05	Anti-symmetry vertical bending+ Symmetrical torsion
Ninth	24.65	Lateral movement+ Anti-symmetry torsion
Tenth	25.94	Anti-symmetry lateral bending+ Anti-symmetry torsion

4.2 Response analysis of wheel excitation non-uniform effect to bridge vibration

4.2.1 Algorithm verification

Fig. 4 shows the RMS curve of the displacement at mid-span point A under the three effects at the heavy vehicle running speed of 60km/h, which was compared with that obtained by the Monte Carlo method using 100 and 500 samples, respectively. From the figure, the RMS curve of displacement simulated using Monte Carlo fluctuated up and down the non-uniform effect curve, verifying the correctness of the method proposed in this study. The calculation results were not remarkably different with the 100 and 500 sample points. At this running speed, the RMS value of displacement under the non-uniform effect was evidently lower than that under the uniform effect, and the coherent effect curve showed a consistent trend with the time lag effect curve. By contrast, the only difference was that the response value of the former was slightly higher than that of the latter.

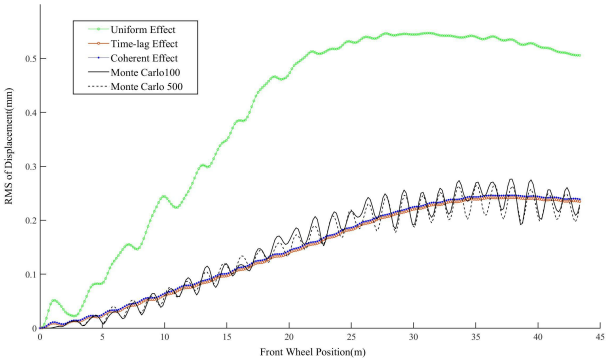

Fig. 4. Comparison curve of RMS response value of mid-span vertical displacement under three effects at the speed of 60km/h

4.2.2 Influence of the vehicle speed

Fig. 5 shows the vehicle speed-dependent change curve of the maximum RMS of side beam mid-span displacement and acceleration. As seen from Fig. 5(a), the RMS of side beam mid-span displacement caused by B-class bridge deck irregularity varied with the vehicle speed, without a monotonic increasing or decreasing relationship between them. At the same running speed, the response value under the non-uniform effect was constantly lower than that under the uniform effect, the maximum response ratio occurred at the running speed of 50km/h, and the former was 0.299 times of the latter. In addition, the response value of the time lag effect curve and that of the coherent effect curve basically overlapped at a speed lower than 80km/h. However, when the speed was higher than 80km/h, the response value of the coherent effect curve was slightly higher than that of the time lag effect curve, but the overall difference was minor. At the running speed of 60km/h, the response value under the non-uniform effect reached a high peak value, whereas the RMS response of displacement reached the minimum value. As known from Fig. 5(b), the running speed-dependent change curve of the maximum RMS of acceleration did not show any monotonic increasing or decreasing relationship. At the same running speed, the response value under the non-uniform effect was consistently lower than that under the uniform effect, the minimum response occurred at a running speed of 50km/h, the former was 0.348 times of the latter, and their response ratio was greater than the ratio of the maximum RMS of displacement. As also observed from Fig. 5(b), the maximum RMS of acceleration under the non-uniform effect changed more evidently with the vehicle speed as that under the uniform effect, and the response value of the time lag effect and that of the coherent effect curve basically overlapped at a speed lower than 80km/h. When the vehicle speed was higher than 80km/h, a slight difference was observed between the coherent effect curve and the time lag effect curve, but the overall difference was minimal. At a vehicle speed of 60km/h, the RMS of displacement under the non-uniform effect had a relatively high peak value, whereas the RMS response of acceleration under the uniform effect reached the minimum value. This finding coincided with the conclusion in Fig. 5 (a).

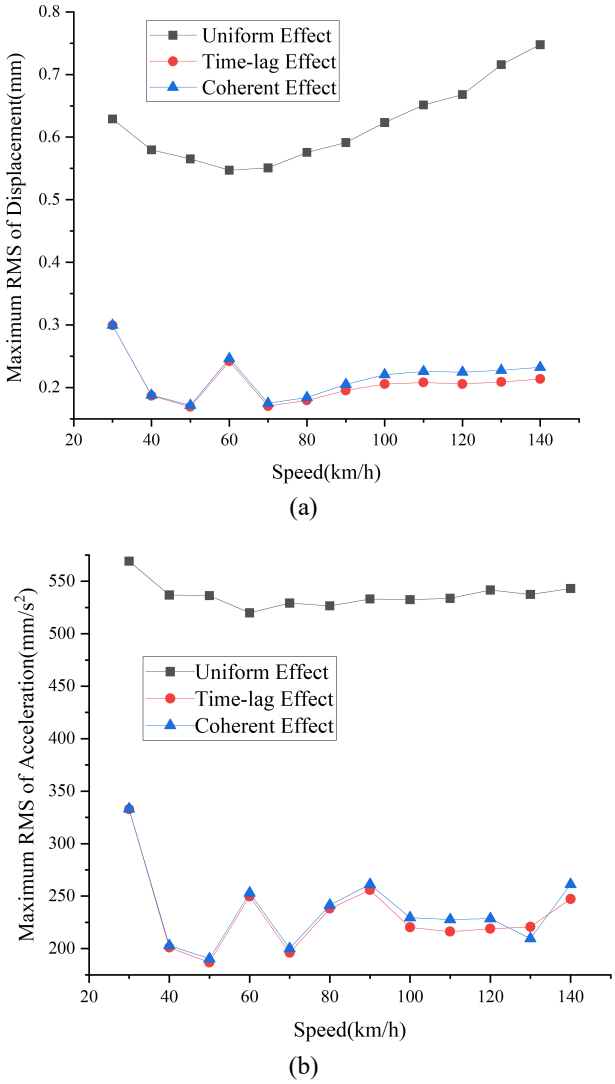

Fig. 5. Curve of the maximum RMS value of mid-span displacement and acceleration varies with the speed. (a)Displacement. (b) Acceleration

Fig. 6 exhibits the vehicle speed-dependent change curves of the front wheel driving position corresponding to minor difference between the acceleration response curves of the two. Table 4 shows the main peak frequency values frequencies corresponding to the main peak PSD with different speeds. From Table 4, the spectral distribution of PSD under the uniform effect did not change with the running speed; whereas under the non-uniform effect, at the vehicle speed of 40km/h, 50km/h, and 80km/h, in addition to the peaks appearing near the first and second frequencies at 3.8Hz and 5.4Hz, a large peak also appears at the frequency of 15.9HZ, which is the fourth order frequency of simply supported beam bridges. At the running speed of 90km/h, the maximum value of PSD under the non-uniform effect only occurred within 5.8–6.1 Hz, which was close to the second-order frequency of the bridge. The above results reveal that when the non-uniform effect is considered, the acceleration response spectrum distribution of the bridge will change due to the change in vehicle speed.

the maximum RMS of side beam mid-span displacement and acceleration. From Fig. 6(a), when the vehicle speed was greater than 60km/h, the driving position of the front wheel corresponding to the maximum response value under the non-uniform effect was later than that corresponding to the maximum response value under the uniform effect at the same running speed. When the speed was higher than 90 km/h, the difference between the two was gradually enlarged. At the running speed of 40km/h, namely, when the front wheel of the second axle ran off the bridge deck, the front wheel driving positions corresponding to the maximum RMS of displacement under the three effects overlapped. At the running speed of 50km/h, the front wheel driving position corresponding to the minimum response value under the non-uniform effect reached a minimum value of 28.9m, namely, when the front wheel was set to leave the bridge deck. From Fig. 6 (b), at the running speed of 30–60 km/h and 90–140km/h, the front wheel driving position upon the maximum response value under the non-uniform effect was earlier than that corresponding to the maximum response value under the uniform effect at the same running speed. As seen from Fig. 6(b), the front wheel driving positions corresponding to the maximum RMS of acceleration under the three effects overlapped at a vehicle speed of 30km/h and 60km/h, i.e., when the second-axle front wheel ran off the bridge deck, and 130km/h, i.e., the rear-axle front wheel ran off the bridge deck. As shown in Fig. 6, the time lag effect curve and the coherent effect curve basically overlapped at other speeds except the slight difference at individual speeds (80 and 90km/h).

4.2.3 Power spectrum analysis of bridge vibration response

Fig. 7 shows the acceleration PSD diagram of mid-span point A at the vehicle speed of 40km/h under the action of the heavy vehicle considering the non-uniform effect. From Fig. 7, the amplitude of PSD under non-uniform effect is significantly lower than that under uniform effect. Meanwhile, no evident differences were observed in the PSD diagram of acceleration between the time lag effect and the coherent effect, which could also be concluded from the

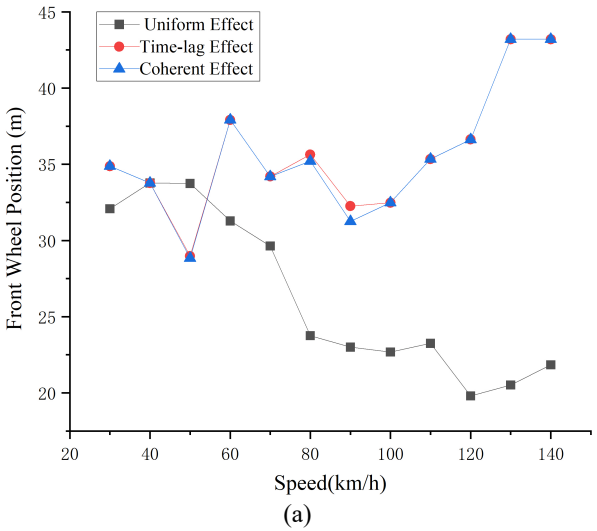

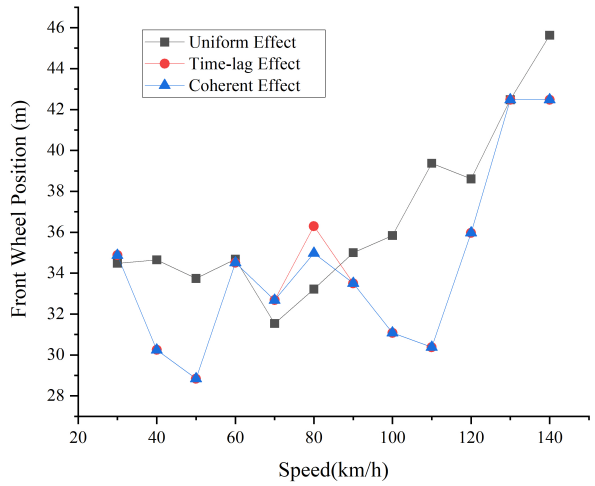

(b)

Fig. 6. Curves of the front wheel driving position corresponding to the maximum value of the RMS of mid-span displacement and acceleration varies with the speed. (a) Displacement. (b) Acceleration

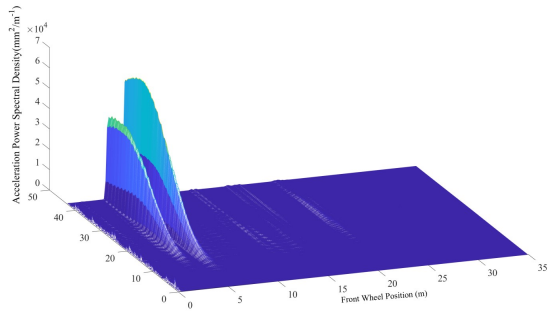

(a)

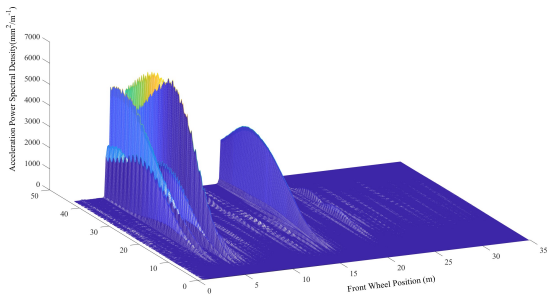

(b)

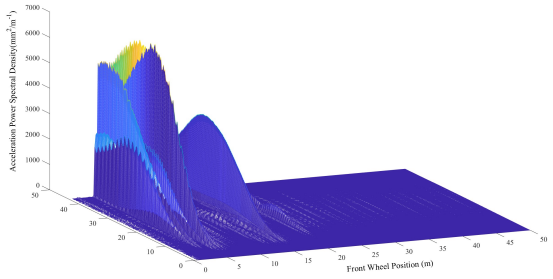

(c)

Fig. 7. Three dimension PSD curves of acceleration caused by uniform and non-uniform excitations at point A at the speed of 40km/h. (a) Uniform effect. (b) Time-lag effect. (c) Coherent effect

Table 4. Frequencies corresponding to the main peak PSD with different speeds

Speed (*Km / h*)	**Main Peek Frequency** (*Hz*)	
	Uniform effects	**Coherent effects**
40	4.2, 5.8	4.3,5.9,15.9
50	4.2,5.8	3.8-4.2,5.8-6.1,15.9
60	4.2,5.8	4.2,5.9
80	4.2,5.8	5.2-6.0,15.9
90	4.2,5.8	5.8-6.1
100	4.2,5.8	3.6-4.0,5.6-6.9
120	4.2,5.8	3.5,4.3-4.7,6.2,15.9

5. Conclusions

To accurately grasp the influence of a six-axle heavy vehicle on the dynamic characteristics of the bridge considering the non-uniform effect of the road surface, a vehicle-bridge coupling random vibration model was established on the basis of the principle of dynamics. The load caused by the road surface irregularity was equivalent to a pseudo-excitation, and the coherent effect model of the road surface excitation under the action of the six-axle heavy vehicle was deduced. The influences of the six-axle heavy vehicle on the vibration and frequency spectrum characteristics of a 30-m simply supported beam bridge considering the non-uniform effect at different driving speeds were explored, and the following conclusions were drawn:

(1) The response values of displacement and acceleration in the bridge mid-span are obviously lower than the response only considering the uniform effect.

(2) The position of the front wheel of the vehicle on the bridge is changed upon the maximum vibration response of the bridge mid-span compared with the result only considering the uniform effect.

(3) The spectral distribution of bridge acceleration response under the non-uniform effect differs from that under the uniform effect, accompanied by the substantial decrease in the amplitude of acceleration PSD.

This study probed the vibration response of a simply supported beam bridge under the action of a six-axle heavy vehicle and investigated the influences of the driving speed on its vibration response and spectrum characteristics, which could truly reflect the real situation when the heavy vehicle passed the simply supported beam bridge. These findings provide theoretical guidance for the dynamic performance analysis of bridges.

However, the current research results are limited to full-load vehicles. Future research can help further judge the dynamic response of simply supported beam bridges by investigating the influences of the change in the load weight of heavy vehicles and their driving speed on the random response and spectrum characteristics of simply supported beam bridges.

Acknowledgements

The authors are grateful for the support provided by National Natural Science Foundation of China (12062006).

References

[1] G. T. Michaltsos and T. G. Konstantakopoulos, "Dynamic response of a bridge with surface deck irregularities," *J. Vib. Control.*, vol. 6, no. 5, pp. 667-689, Jul. 2000.

[2] R. Y. Rubinstein and D. P. Kroese, *Simulation and the Monte Carlo method*. New York, NY, USA: John Wiley & Sons, 2016.

[3] P. Múčka, "Simulated road profiles according to ISO 8608 in vibration analysis," *J. Test. Eval.*, vol. 46, no. 1, pp. 405-418, Jan. 2017.

[4] J. Lin, W. Zhang, and J. Li, "Structural responses to arbitrarily coherent stationary random excitations," *Comput. Struct.*, vol. 50, no. 5, pp. 629-633, Mar. 1994.

[5] P. A. Montenegro, J. M. Castro, R. Calcada, J. M. Soares, H. Coelho, and P. Pacheco, "Probabilistic numerical evaluation of dynamic load allowance factors in steel modular bridges using a vehicle-bridge interaction model," *Eng. Struct.*, vol. 226, pp. 111316, Jan. 2021.

[6] P. Sivaramakrishnan, A. K. M. Prakash, D. Sekulic, B. Jacobson, C. Selvi, and S. M. Johannesen, "Methods to introduce floating bridge motion and wind excitation on a model for the investigation of heavy vehicle dynamics," *Appl. Math. Model.*, vol. 117, pp. 118-141, May 2023.

[7] M. W.Meyer, D.Cantero, and R. Lenner, Dynamics of long multi-trailer heavy vehicles crossing short to medium span length bridges. *Eng. Struct*, vol. 247, 15 Nov. 2021, Art. no. 113149

[8] A. P. Pagnoncelli and L. F. F. Miguel, "Methodology to obtain dynamic response of road bridges considering bridge–vehicle interactions," *Pract. Period. Struct.*, vol. 24, no. 3, Apr. 2019, Art. no. 04019010.

[9] G. Lombaert and J. P. Conte, "Random vibration analysis of dynamic vehicle-bridge interaction due to road unevenness," *J. Eng. Mech.*, vol. 138, no. 7, pp. 816-825, Jul. 2012.

[10] P. Asnachinda, T. Pinkaew, and J. A. Laman, "Multiple vehicle axle load identification from continuous bridge bending moment response," *Eng. Struct.*, vol. 30, no. 10, pp. 2800-2817, Oct. 2008.

[11] B. Nunia, M. Koli, S. Pandey, S. Naik, and A. K. Dixit, "Computational model on influence of prestress level on vehicle-bridge coupled vibrations," *Int. J. Interact. Des. Manuf.*, pp. 1-13, Jan. 2023.

[12] B. Nunia, T. Rahman, S. Choudhury, and P. Janardhan, "Effect of vehicle speed and road surface roughness on the impact factor of simply supported bridges due to IRC Class A and B loading," *SN Appl. Sci.*, vol. 2, pp. 1-24, Apr. 2020.

[13] O. Mohammed, A. Gonzalez, and D. Cantero, "Dynamic impact of heavy long vehicles with equally spaced axles on short-span highway bridges," *Balt. J. Road Bridge E.*, vol. 13, no. 1, pp. 1-13, Mar. 2018.

[14] H. Ho and M. Nishio, "Evaluation of dynamic responses of bridges considering traffic flow and surface roughness," *Eng. Struct.*, vol. 225, Dec. 2020. Art. no. 111256.

[15] G. Alencar, A. M. de Jesus, R. A. Calçada, and J. G. S. da Silva, "Fatigue life evaluation of a composite steel-concrete roadway bridge through the hot-spot stress method considering progressive pavement deterioration," *Eng. Struct.*, vol. 166, pp. 46-61, Jul. 2018.

[16] J. Oliva, J. M. Goicolea, P. Antolín, and M. Á. Astiz, "Relevance of a complete road surface description in vehicle–bridge interaction dynamics," *Eng. Struct.*, vol. 56, pp. 466-476, Nov. 2013.

[17] C. C. Caprani, "Application of the pseudo-excitation method to assessment of walking variability on footbridge vibration," *Comput. Struct.*, vol. 132, pp. 43-54, Feb. 2014.

[18] S. Tamaddon, M. Hosseini, and A. Vasseghi, "Effect of non-uniform vertical excitations on vertical pounding phenomenon in continuous-deck curved box girder RC bridges subjected to near-source earthquakes," *J. Earthq. Eng.*, vol. 26, no. 10, pp. 5360-5383, Feb. 2022.

[19] H. Tang, Y. Li, K. M. Shum, X. Xu, and Q. Tao, "Non-uniform wind characteristics in mountainous areas and effects on flutter performance of a long-span suspension bridge," *J. Wind Eng. Ind. Aerod.*, vol. 201, Jun. 2020, Art. no. 104177.

[20] G. Bethel Lulu, R. Chen, P. Wang, J. Xu, J. Chen, and J. Fang, "Random vibration analysis of tram-track interaction on a curve due to the polygonal wheel and track irregularity," *Vehicle SysT. Dyn.*, vol. 60, no. 4, pp. 1125-1147, Dec. 2022.

[21] C. Ma and D. H. Choi, "Random dynamic analysis of the train-track-bridge system under tridirectional spatially correlated ground motions," *Soil Dyn. Earthq. Eng.*, vol. 160, Sep. 2022. Art. no. 107324.

[22] Z. Zembaty, "Vibrations of bridge structure under kinematic wave excitations," *J. Struct. Eng.*, vol. 123, no. 4, pp. 479-488, Apr. 1997.

[23] W. Han, Y. Yuan, P. Huang, J. Wu, T. Wang, and H. Liu, "Dynamic impact of heavy traffic load on typical T-beam bridges based on WIM data," *J. Perform. Constr. Fac.*, vol. 31, no.3, Jun. 2017. Art. no. 04017001.

[24] S. Narayanan, *Nonlinear and Nonstationary Random Vibration of Hysteretic Systems with Application to Vehicle Dynamics*. Berlin Brandenburg, Germany: Springer Berlin Heidelberg, 1988.

[25] P. H. Wirsching, T. L. Paez, and K. Ortiz, *Random vibrations: theory and practice*. New York, NY, USA: Dover Publications, Inc., 2006.